Journal of Catalysis **206,** 331–338 (2002)
doi:10.1006/jcat.2001.3499, available online at http://www.idealibrary.com on IDEAL®

Molecular-Level Insight into Cr/Silica Phillips-Type Catalysts: Polymerization-Active Dinuclear Chromium Sites

Øystein Espelid and Knut J. Børve

Department of Chemistry, University of Bergen, Allégaten 41, N-5007 Bergen, Norway
E-mail: oystein.espelid@kj.uib.no; knut.borve@kj.uib.no

Received September 13, 2001; revised December 13, 2001; accepted December 15, 2001

Prospects of ethylene polymerization over dinuclear Cr(II) sites of the reduced Cr/SiO_2-based Phillips catalyst have been investigated by means of cluster models and gradient-corrected density functional theory. The starting structure for polymerization is considered to arise through reactions between ethylene and the dichromium site. A feasible route is found to a structure with a butano moiety suspended between the two chromium centers. The bridging alkano ligand may grow by facile insertion of ethylene into either of the chromium–carbon bonds. The relative rates of monomer insertion and termination through β-hydrogen transfer, as a function of the length of the bridging organic ligand, agrees with the production of 1-hexene observed during early stages of polymerization.

Key Words: **polymerization; ethylene; Phillips catalysis; density functional theory; initiation; propagation; cluster models.**

1. INTRODUCTION

The past few years have witnessed a resurgence in fundamental research aimed at elucidating structural (1–5) and mechanistic aspects (3, 6, 7) of Phillips catalysis (8). This inorganic Cr/silica system maintains its position among catalysts for producing polyethylene, due to the possibility of varying the properties of the produced polymer through the choice of support and preparation procedure (2, 9). While useful during production, this property complicates fundamental research, as does the fact that only a small fraction of the chromium is actually active with respect to polymerization (8).

Prior to polymerization, standard Phillips catalysts exhibit chromium mainly in oxidation state II and anchored onto silica by ester oxygen linkages on a highly dehydroxylated surface (8). McDaniel and Welch concluded that conventionally prepared Phillips catalysts have two kinds of active sites, producing high and low molecular weight (MW) polymer, respectively (10). The activity of the catalyst was shown to correlate with the calcination temperature (T_c). The observed increase in activity with T_c was accompanied by a decrease in the MW of the polymer, attesting to an increased termination rate relative to that of propagation (10). In the range of increasing activity, the hydroxyl population decreased, without actually reaching zero (10). Complete removal of surface hydroxyls, e.g., by fluorination, allows for highly active Phillips-type catalysts (8). However, this patented modification unexpectedly produced high MW polymer with a narrow MW distribution (10).

Ruddick and Badyal investigated formation and desorption of byproducts and observed only fully deuterated 1-hexene mass fragments when their pre-reduced catalyst was exposed to C_2D_4 (11). As the formation of 1-hexene was limited to the early stages of polymerization, the sites responsible for trimerization were proposed active also for polymerization (11). Selective trimerization and polymerization of ethylene is expected to proceed *via* metallacyclic intermediates (11). In Ruddick and Badyal's study (11) as well as in the case of fluorinated catalysts (8), it appears that the starting structure for polymerization must evolve in a reaction between ethylene and chromium of the reduced catalyst.

Carbon monoxide has been used as probe molecule to differentiate chromium sites with respect to coordination environment and acidity (12–15). Theoretical analysis of carbonyl infrared spectra was used to reassign spectra of the reduced Cr/silica system, pointing to appreciable amounts of both dinuclear and mononuclear chromium(II) surface species (5). On the other hand, based on ion-scattering experiments on a surface-science model of the catalyst, it was concluded that only monochromate esters are present at low chromium loading (16). The lack of pores and internal surfaces in the thin-film amorphous silica support used in the model makes it difficult to generalize this result to Phillips catalysts. Thus, while it certainly topicalizes mononuclear sites as active for polymerization, the possibility for dinuclear sites should not be dismissed.

In recent work, we investigated the prospects of ethylene polymerization over mononuclear Cr(II) sites (6, 7). Mononuclear coordinatively unsaturated Cr(II)-A-type sites were found unable to assist ethylene polymerization in Phillips-type catalysts, as they inevitably lead to inert four-coordinated Cr(IV) species with tetrahedral arrangement

0021-9517/02 $35.00

of ligands (6, 7). However, hydrogen transfer from a coordinating silanol group was found to afford activation, provided that the silica matrix offers a minimum of strain to prepare the resulting structure for ethylene coordination (7). Such an activated B-type site displays a linear starting polymer chain, the formation of which requires hydrogen from a surface silanol group (7). Thus, it is seemingly unable to account for the observations made by Ruddick and Badyal (11).

The issue of how an initial monoalkylchromium structure may be generated without external alkylating agents has been discussed in the literature (2, 8, 17). Rebenstorf (17) suggested that the growing polymer chain may be suspended between the chromium atoms of a dinuclear site. This would leave each chromium in a monoalkyl configuration, yet alleviate the need for additional hydrogen atoms. In the present contribution, we follow up the suggestion by Rebenstorf and apply quantum chemical methods in conjunction with cluster models, to examine the prospect of ethylene polymerization at a dinuclear site. Furthermore, the propensity for trimerization as observed in the Phillips catalyst by Ruddick and Badyal (11) is investigated. As far as the initiation mechanism is concerned, focus is put on mechanisms leading to the starting structure for polymerization proposed by Rebenstorf. The present contribution is fully within the concept of coordinative unsaturated dinuclear chromium sites (15).

2. COMPUTATIONAL DETAILS

The study was conducted using gradient-corrected density functional theory as implemented in the Amsterdam Density Functional (ADF) set of programs (18, 19). For the correlation functional, the local potential by Vosko *et al.* (20) and the nonlocal 1986 correction by Perdew (21) were used. The exchange functional consisted of the Slater term augmented by gradient corrections as specified by Becke (22). Extensive studies (23) demonstrate that the resulting energy functional is capable of providing accurate energy profiles for the insertion step during metal-catalyzed olefin polymerization. For later reference, the change in energy was computed for the organic reaction *ethylene* + *ethane* → *n-butane* to be −98 kJ/mol.

Closed- and open-shell systems were described within spin-restricted and -unrestricted formalisms, respectively. Primitive Slater-type basis sets of triple-zeta (O,F,Cr) and double-zeta (H,C,Si) quality were used as supplied with ADF and detailed in Ref. (6), with polarization functions added to all atoms but chromium. Molecular geometries were converged to a gradient below 0.001 E_H/Å with the accuracy of the numerical integration schemes adjusted accordingly. Transition-state optimization was conducted as described in Ref. (6). Energy differences refer to electronic degrees of freedom, i.e., without inclusion of zero-point vibrational energies.

The electronic ground state of the low-valent chromium species were consistently found to be high-spin coupled. The magnitude of the basis set superposition error (BSSE) within the presently applied computational model was examined for the ethylene-chromium π-complex shown as **1a** in Fig. 2. In the geometry realized in **1a**, the energy of ethylene is lowered by 6.5 kJ/mol by inclusion of the full (ghost) basis set belonging to the $\mathbf{D_n}$ cluster. The corresponding number for the cluster in the presence of the ghost basis set for ethylene is 1.1 kJ/mol. This implies a counter-poise correction of 7.6 kJ/mol to a binding energy of 40 kJ/mol, which is regarded as acceptable.

3. CLUSTER MODELS

The Phillips catalyst is commonly prepared by impregnating CrO_3 on silica (8), followed by heating in an oxygen-rich atmosphere. During calcination, chromium is expected to anchor onto silica in a condensation reaction with two neighboring surface silanols. Chromium is mainly present in a hexavalent state, anchored to silica through oxygen linkages as chromate and dichromate esters (24). Upon contact with ethylene, the anchored hexavalent chromium species are expected to become reduced to their divalent analogs.

Dinuclear chromium(II) sites were modeled by the two cluster models presented in Fig. 1. They may be regarded as -OCrOCrO- moieties anchored to sites of narrow ($\mathbf{D_n}$) and intermediate-to-wide ($\mathbf{D_w}$) "bites," see Ref. (5). The use of two clusters is considered useful to probe the sensitivity of the results with respect to the choice of cluster model.

Starting from dichromic acid, the anchoring reaction to the sites with narrow and intermediate-to-wide bites were calculated to be endothermic by 8 and 19 kJ/mol, respectively. Taking into account the entropic driving force of the reaction, the dichromate precursors to the $\mathbf{D_n}$ and $\mathbf{D_w}$ clusters appear as likely products in the calcination step. Reduction to divalent species may be achieved in a separate pretreatment step with carbon monoxide (25). Reduction by carbon monoxide to obtain the divalent $\mathbf{D_n}$ and $\mathbf{D_w}$ cluster models from their dichromate precursors were computed to

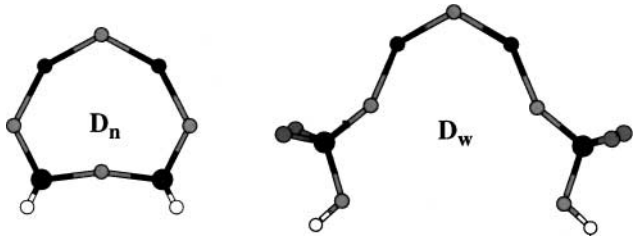

FIG. 1. $\mathbf{D_n}$ ($Cr_2O_4(SiH_2)_2$) and $\mathbf{D_w}$ ($Cr_2O_3(SiF_2OH)_2$) dinuclear cluster models. The elements are coded on a gray scale according to increasing atom number H (white) < O < F < Si < Cr (dark gray).

be exothermic by 190 and 262 kJ/mol, respectively. While this supports dichromium(II) species as a product in the reduction step, it is conceivable that the reduction may stop at a higher oxidation state. In fact, a minor population of chromium(III) surface species has been reported to be present at the reduced catalyst, and dichromium(III) species with two oxygen bridges between the chromium centers are among the proposed structures (26). However, reduction of the dichromium(III) analog to the divalent $\mathbf{D_w}$ cluster by carbon monoxide was calculated to be exothermic by 40 kJ/mol. Thus, the equilibrium of the dichromium species seems to be shifted toward the divalent species, at least when exposed to carbon monoxide. The energy contribution from relativistic effects is expected to decrease the estimate of the heat released during reduction (27), without altering the order of stability.

Both the $\mathbf{D_n}$ and $\mathbf{D_w}$ cluster models are constructed with an understanding that the surrounding silica matrix limits to some extent the structural flexibility of the anchoring site. Thus, to maintain a wide-bite $\mathbf{D_w}$ cluster and prevent excessive geometric relaxation, the Si–Si distance was frozen (at 7.0 Å) and only the –OCrOCrO– moiety was allowed to relax geometrically. The cyclic structure of the narrow-bite $\mathbf{D_n}$ cluster model naturally presents limited flexibility. The $\mathbf{D_n}$ cluster was used extensively to investigate the initiation phase, in which H atoms were used as terminating agents to limit the computational cost. The more elaborate $\mathbf{D_w}$ cluster is invoked when considering propagation and β-hydrogen termination. The acidity of the chromium centers in this cluster model is considered more realistic, due to the improved acidity (1430 kJ/mol) of the corresponding silanol groups of the anchoring site.

4. RESULTS

4.1. Initiation

Adsorption of the first ethylene. Ethylene is found to form a donation bond of 40 kJ/mol to either of the chromium atoms at the dinuclear $\mathbf{D_n}$ site, see structure **1a** in Fig. 2. This structure acts as a precursor to a covalently bound complex which is realized at a closer approach of ethylene to chromium, see **1b** in Fig. 2. The net charge on the active chromium atom increases significantly, reflecting the change in formal oxidation state from Cr(II) to Cr(IV). In turn, the bridging oxygen ligand is pulled closer to the more positive Cr and displays inequivalent Cr–O bond lengths of 1.70 and 1.84 Å. The chromium–carbon distance is down to 2.03 Å and the carbon–carbon bond is stretched to 1.44 Å. The energy of the covalently bound ethylene complex is computed to −85 kJ/mol relative to that of free reactants. A third coordination mode is available in which ethylene is suspended between the two chromium atoms, cf. **1c** in Fig. 2. In this structure, which is stable by 82 kJ/mol relative to free reactants, each chromium is in oxidation state III. The complex is best described as a μ-ethano-μ-oxo-dichromium structure, with the carbon–carbon bond stretched to 1.51 Å and with chromium–carbon bond lengths of 2.06 Å.

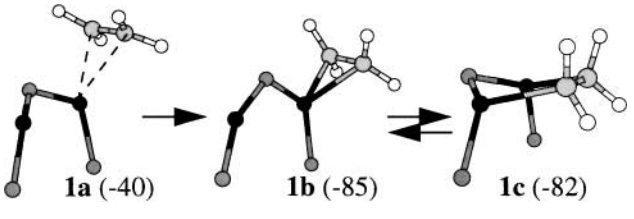

FIG. 2. Three different coordination modes of ethylene at a dinuclear site: **1a** Molecular coordinated ethylene; **1b** Covalent coordinated ethylene; **1c** Covalently bound ethylene suspended between the chromium centers. The elements are coded on a gray scale according to increasing atom number.

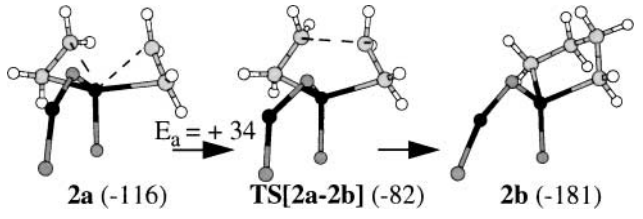

FIG. 3. Cycloaddition reaction of two ethylene molecules coordinated to the same chromium atom, with a precursor π complex **2a**, transition state **TS[2a–2b]** and chromacyclopentane product **2b**, as obtained with the $\mathbf{D_n}$ cluster model. The elements are coded on a gray scale according to increasing atom number.

Adsorption of a second ethylene. Starting from either **1b** or **1c**, there are a number of possible diethylene complexes resulting from the adsorption of an additional molecule of ethylene to either of the two chromium atoms. Figure 3 illustrates the adsorption of a second monomer to the chromium atom ($Cr^{(1)}$) that is already covalently bound to the first ethylene in **1b**. The spin is conserved as the second ethylene binds to form structure **2a**, with an energy of coordination of −31 kJ/mol. The low complexation energy results from a reduction in ionic interaction between $Cr^{(1)}$ and the bridging oxygen as the net charge on the oxidized chromium is reduced upon the second ethylene coordination. A low energy barrier of 34 kJ/mol separates **2a** from forming the related chromacyclopentane structure, **2b** in Fig. 3. The cycloaddition reaction was found to be exothermic by 99 kJ/mol, leaving **2b** at an energy of −181 kJ/mol relative to two ethylene molecules and the reduced cluster. The transition state **TS[2a–2b]** along the reaction path of cycloaddition was located at a forming carbon–carbon distance of 2.04 Å.

Alternatively, a second ethylene may adsorb onto the chromium atom adjacent to $Cr^{(1)}$, henceforth denoted by $Cr^{(2)}$. In structure **2c** in Fig. 4, the second ethylene forms a donation bond of 44 kJ/mol to $Cr^{(2)}$. Additional 9 kJ/mol

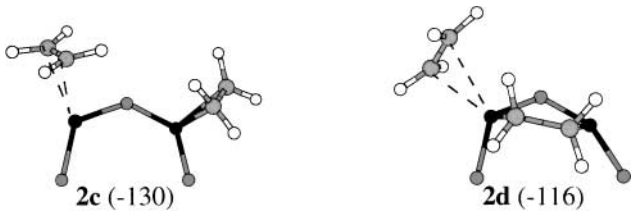

FIG. 4. Ethylene molecularly coordinated to a dichromium site with either an additional covalently bound ethylene (**2c**) or a μ-ethano ligand (**2d**), obtained with the $\mathbf{D_n}$ cluster model. The elements are coded on a gray scale according to increasing atom number.

is gained in stability by converting to covalent coordination mode also for the second monomer, implying a change in spin state to feature both chromium atoms in oxidation state IV.

Finally, a second ethylene is found to coordinate molecularly to the μ-ethano complex **1c**, with an energy of −35 kJ/mol. This structure is included as **2d** in Fig. 4.

While the energy gain from fusing two ethylene moieties makes the chromacyclopentane structure **2b** the most stable encountered thus far, the tetrahedral arrangement of ligands about $Cr^{(1)}$ renders **2b** an unlikely starting point for further reactions with ethylene (6). On the other hand, the analogous μ-butano structure **3a** in Fig. 5, formally obtained by allowing one of the α-carbons in **2b** to migrate to the adjacent divalent chromium center, is essentially isoenergetic with the chromacyclopentane species, at an overall stability of −174 kJ/mol relative to isolated monomers and the naked cluster. Moreover, this structure displays two chromium(III)-alkyl coordination sites, the chemistry of which is examined in following sections.

Two different reaction paths for the preparation of **3a** have been examined, starting from **2d** and **2b**, respectively. The μ-butano-μ-oxo-dichromium structure was attempted formed by inserting the molecularly coordinated ethylene in **2d** into the nearest covalent Cr–C bond. The appropriate nonbonding C–C distance was gradually reduced while relaxing all other degrees of freedom. This effort served only to induce a migration of the μ-ethano fragment, to produce structure **2a**. It is already shown how **2a** may act as a precursor to the chromacyclopentane structure **2b**. Our second attempt involved the migration of one of the α-carbons in **2b** to the adjacent divalent chromium center. This intramolecular transformation implies Cr–C bond cleavage on the initial chromium ($Cr^{(1)}$), and Cr–C bond formation on adjacent $Cr^{(2)}$. This possibility was examined by gradually reducing the distance between $Cr^{(2)}$ and an α-carbon, while relaxing the remaining degrees of freedom. The initial region of the linear transit scan describes Cr–C bond cleavage in chromacyclopentane, without any sign of bond formation to the adjacent chromium. The energy increases gradually and passes through a maximum approximately 50 kJ/mol above the energy of structure **2b**. Past the maximum, the $Cr^{(2)}$–C_α bond manifests itself almost abruptly, and the energy drops dramatically. This close-to discontinuous energy profile indicates an insufficient description of the transition-state region, most likely due to multiconfigurational effects but possibly also due to a less-than optimal choice of the internal coordinate used to drive the reaction path. In any case, we expect that improving these deficiencies would act to stabilize the transition region relative to reactant and product, and therefore that structure **3a** should be regarded as a topical intermediate for further reactions. Each chromium is trivalent and in oxidation state III. The chromium–carbon bonds have single-bond character as evident from bond lengths of 2.02–2.03 Å. The chromium–oxygen bond lengths are 1.78 and 1.81 Å, for the oxygen bridging each chromium to another chromium and silicon, respectively. The distance between the two chromium centers is 3.07 Å.

Formation of μ-hexano-μ-oxo-dichromium(III). An incoming monomer may coordinate molecularly to either of the chemically equivalent chromium atoms in the μ-butano structure, cf. **3b** in Fig. 5. The coordination energy is a mere −21 kJ/mol, corresponding to Cr–C distances of 2.6 and 2.8 Å. Accordingly, the carbon–carbon double bond is barely affected at all, while the adjacent covalent chromium–butano bond is stretched to 2.05 Å.

The transition state for insertion of ethylene into the adjacent Cr–C bond, **TS[3b–3c]** in Fig. 5, is located at a carbon–carbon distance of 2.09 Å, and constitutes a barrier of 43 kJ/mol relative to the π complex. The length of the forming chromium–carbon bond is down to 2.05 Å, while

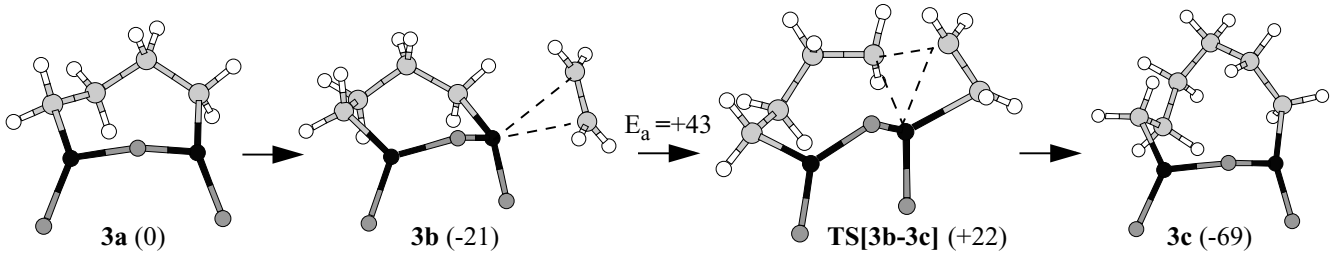

FIG. 5. Insertion of ethylene into the Cr–C single bond of a μ-butano-μ-oxo-dichromium structure **3a**, with π complex **3b**, transition state **TS[3b–3c]**, and product **3c**, as obtained with the $\mathbf{D_n}$ cluster model. The elements are coded on a gray scale according to increasing atom number.

the chromium–carbon bond to be broken is stretched to 2.24 Å. Together with the ethylene bond length of 1.44 Å, these geometry parameters indicate a late transition state.

Considering the cyclic structure composed of the alkano ligand together with the Cr–O–Cr segment, the reactant **3a** and product **3c** constitute seven and nine-membered rings, respectively. The energy change associated with extending the bridging alkano ligand from four to six carbons atoms is computed to −69 kJ/mol. This is 29 kJ/mol less exothermic than computed for the reference reaction of preparing n-butane from ethane and ethylene, cf. *Computational Details*, and this deviation matches well the known difference in ring strain between cyclononane and cycloheptane (28).

4.2. Formation of 1-Alkene Oligomers

Formation of 1-hexene from the μ-hexano structure **3c** in Fig. 5 is examined along the path of β-hydrogen transfer. The atoms in the Cr–C–C–H segment initially containing the transferring hydrogen will be denoted as $Cr^{(1)}$, C_α, C_β, and H_β, respectively. At the other end of the alkano ligand, the relevant atoms are denoted by $Cr^{(2)}$ and $C_{\alpha 2}$. Structure **4a** in Fig. 6 shows the reactant in a conformation of pronounced β-agostic interaction, given by a $Cr^{(2)}$–H_β distance of 2.00 Å. The C_β–H_β bond is stretched by approximately 1 pm, and this structure is only 21 kJ/mol less stable than the global minimum, **3c**.

The reaction path corresponds to concerted β-hydrogen transfer, where H_β is transferred from C_β to $C_{\alpha 2}$, see Fig. 6. As the C_β–H_β bond is stretched, C_β coordinates to $Cr^{(2)}$ and a double bond starts to develop between C_α and C_β. In the region prior to the transition state, the budding vinyl moiety binds covalently to both chromium atoms, rather similar to what is found in **1c** of Fig. 2. The $Cr^{(2)}$–$C_{\alpha 2}$ bond lengthens

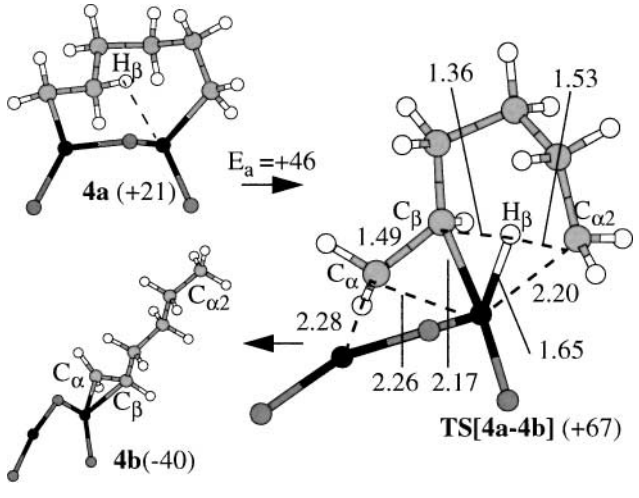

FIG. 6. Concerted β-H transfer reaction in the μ-hexano-μ-oxo-dichromium structure (**4a**), with transition state **TS**[**4a–4b**] and product **4b**, as obtained with $\mathbf{D_w}$ cluster model. The elements are coded on a gray scale according to increasing atom number.

in concert with the translation of the β-hydrogen within the coordination sphere of $Cr^{(2)}$. Selected geometry parameters of the transition state **TS**[**4a–4b**] are presented in Fig. 6. C_α is suspended between the two chromium centers in the transition state, and the C_α–C_β vinyl moiety tends to coordinate to $Cr^{(2)}$. Thus, the product is expected to be a covalently coordinated 1-hexene, corresponding to structure **1b** in Fig. 2. This view is supported by the net charges and the spin at the chromium centers in the **TS**[**4a–4b**] transition state structure. In the reactant **4a**, both chromium centers have a formal oxidation number of III, while in the transition state and the product, the catalytic chromium center $Cr^{(2)}$ is in oxidation state IV, leaving the other chromium in oxidation state II. From the product, structure **4b**, 1-hexene may undergo a transformation to molecular coordination, corresponding to structure **1a** in Fig. 2, to be subsequently displaced by an incoming ethylene monomer, thereby releasing 1-hexene to the gas phase.

The **TS**[**4a–4b**] transition state constitutes an energy barrier of 46 kJ/mol, relative to structure **4a**. However, relative to the most stable conformation of the reactant, the apparent $\Delta H^\ddagger$ is calculated to 67 kJ/mol, and the overall reaction exothermicity to structure **4b**, is calculated to be 40 kJ/mol.

In **TS**[**4a–4b**], a six-membered ring is formed by the catalytic chromium atom together with most of the carbon backbone, leaving out only the $OCr^{(1)}C_\alpha$ moiety, i.e., the bridging oxygen, the spectator chromium, and the α-carbon. In organic chemistry, ring strain in cycloalkanes is measured relative to that of cyclohexane, for which it is defined to be zero (28). The ring strain is known to reach a high for cyclononane, at 53 kJ/mol (28). Applying this perspective to the present metallacyclic structures, the strained nine-membered cyclic reactant **3c** is seen to facilitate a transition state that displays a chromacyclohexane unit in the chair conformation. This combination of reactant and transition state structures with notably high and low ring strains, respectively, is unique to the formation of 1-hexene. To viz., if 1-butene were to be formed by the reaction mechanism studied, only starting from the μ-butano structure **3a**, the contribution from ring strain alone is expected to raise the activation energy by 84 kJ/mol, compared to that of the 1-hexene reaction. This follows from the values of ring strain in cyclobutane and cycloheptane, of 110 kJ/mol and 26 kJ/mol, respectively. Correspondingly, in the limit of a very long bridging alkano ligand, the barrier for β-hydrogen termination by this mechanism is expected to be around 120 kJ/mol.

4.3. Propagation

While insertion of ethylene into a Cr–C bond in the μ-butano structure **3a** was described as part of the initiation process, the energetics of this reaction will change as the alkano ligand grows, due to the disappearance of ring strain (28). As a limiting case, relevant to the propagation step

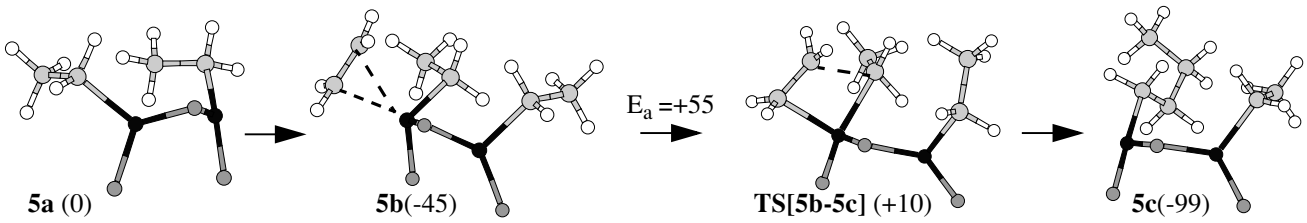

FIG. 7. Insertion of ethylene into a Cr–C single bond in the μ-oxo-di(chromium-ethyl) structure **5a**, with π complex **5b**, transition state **TS[5b–5c]**, and product **5c**, as obtained with the $\mathbf{D_w}$ cluster model. The elements are coded on a gray scale according to increasing atom number.

during polymer growth, ethylene insertion into a Cr–C bond in a μ-oxo-di(ethylchromium) structure is modeled, cf. Fig. 7. The presentation focuses on the results derived from $\mathbf{D_w}$, yet, for comparison, numerical results are complemented by the corresponding values computed for the $\mathbf{D_n}$ cluster within square brackets.

Formation of a molecular ethylene–chromium π complex (**5b** in Fig. 7), is exothermic by -45 kJ/mol [-38 kJ/mol], with ethylene coordinating at chromium–carbon bond distances of 2.25 and 2.51 Å [2.31 and 2.57 Å], and having its double bond stretched to 1.38 Å [1.36 Å]. The transition state, **TS[5b–5c]** is located at a forming carbon–carbon bond distance of 2.11 Å [2.16 Å] and constitutes a barrier of 55 kJ/mol [43 kJ/mol] relative to the π complex. The ethylene double bond is stretched to 1.42 Å [1.42 Å], and the chromium–carbon bonds to be formed and broken are 2.06 and 2.16 Å [2.07 and 2.17 Å], respectively. The insertion is assisted by an α-agostic interaction, evident from a stretch in the C_3–H_α bond of 1.5 pm [0.8 pm], at a Cr–H_α distance of 2.11 Å [2.18 Å]. Furthermore, the chromium–oxygen bond lengths are only moderately affected along the reaction path of insertion. The insertion energy to form the product is -99 kJ/mol [-98 kJ/mol], in close agreement with the organic reference reaction described earlier.

Assuming the presently studied reaction mechanism to be responsible for chain propagation at dichromium sites at the Phillips catalyst, it should be possible to halt the polymerization process by introducing stable molecules that out-compete ethylene with respect to adsorption onto chromium. Such an experiment was in fact carried out by Rebenstorf (29), who introduced CO to and recorded carbonyl infrared spectra of the reduced catalyst as well as after a short time of polymerization. After inlet of ethylene, the difference spectrum shows a broad, positive band centered at 2177 cm^{-1}. This was assigned by Rebenstorf to CO adsorbed at the active site holding the polymer chain. Moreover, polymerization led to the disappearance of a triplet of bands in the region of 2035–2120 cm^{-1}. Using theoretical modeling, we have recently assigned this triplet to oligocarbonyl species at dinuclear sites (5).

To investigate Rebenstorf's observations by theoretical means, CO adsorption to **5a** was considered for the $\mathbf{D_w}$ cluster. Carbon monoxide was found to coordinate to the vacant site at a chromium–carbon distance of 2.04 Å and with a coordination energy of 67 kJ/mol. Since the corresponding binding energy was computed to 45 kJ/mol for ethylene, CO is indeed found to out-compete ethylene as adsorbate. The CO vibrational frequency was calculated to 2050 cm^{-1}, which deviates substantially from the observed maximum in the difference spectrum, at 2177 cm^{-1}. The problem of relating computed carbonyl frequencies to those observed is discussed at length in Ref. (5). Here we adopt the recommended reference state, namely the band that is observed (29) at 2178 cm^{-1} and computed at 2068 cm^{-1} in cluster studies (5). Relative to this reference band, the band associated with polymerization is found experimentally to be red-shifted by 1 cm^{-1}, compared to a red-shift of (2068–2050) cm^{-1} = 18 cm^{-1} with the presently applied computational models. Taking into account the width of the observed band and the limited accuracy of our computational model, the band observed by Rebenstorf (29) may be attributed to CO-arrested active dichromium sites.

5. DISCUSSION

Rebenstorf (17) proposed a μ-ethano-μ-oxo-dichromium starting structure for polymerization. The calculations show a drive toward adsorption of one additional equivalent of ethylene and to form a chromacyclopentane species through carbon–carbon bond fusion. While analogous structures are found for mononuclear sites (6), it is particular to the dichromium site that reorganization to a μ-butano structure seems feasible in a close-to isoenergetic process. However, due to limitations implicit in a single-configurational description of the electronic structure, we are presently not able to present a full reaction path for the formation of μ-butano-μ-oxo-dichromium. Moreover, it is quite possible that our DFT description has a slight bias toward a Cr(II)–Cr(IV) situation over Cr(III)–Cr(III), eventually favoring a chromacyclopentane-based product over one with a μ-butano ligand. Thus, obtaining μ-butano-μ-oxo-dichromium through insertion of ethylene to the corresponding μ-ethano structure should be regarded a viable option.

Subsequent insertion of ethylene into a Cr–C bond in μ-butano-μ-oxo-dichromium is found to proceed with a

modest barrier. The overall heat of reaction is also low, partly due to ring strain in the nine-membered ring structure of the μ-hexano product. The μ-hexano-μ-oxo-dichromium(III) structure may undergo concerted β-hydrogen transfer, with subsequent release of 1-hexene and regeneration of a reduced dinuclear chromium site. The energy barrier for β-hydrogen transfer in the μ-hexano structure is low, partly due to release of ring strain in the nine-membered cyclic reactant as compared to that of the six-membered ring formed at the transition state. In fact, relying on values for ring strain of cycloalkanes (28), β-hydrogen transfer in the μ-butano structure is expected to have a prohibitively high barrier, and also for ring sizes past the hexano structure the reaction barrier is expected to exceed 100 kJ/mol. The 1-hexene thus produced does not contain hydrogen foreign to ethylene. While these predictions are in line with the observation made by Ruddick and Badyal (11), other researchers report formation of a series of 1-alkenes byproducts (3, 30). This can be understood in light of the present results if only dinuclear sites were activated on Ruddick and Badyal's catalyst (11) while mononuclear sites make up a significant fraction of the activated sites when a prolonged series of 1-alkenes are observed (3, 5).

In the μ-hexano structure, the apparent barrier for β-hydrogen transfer is computed at 67 kJ/mol, to be compared to the energy barrier toward monomer insertion of 39 kJ/mol, relative to the π complex. From this, the dinuclear site is predicted to catalyze the formation of polymer over 1-hexene.

In the propagation step as modeled on a μ-oxo-di(ethylchromium) structure, the monoethylene π complex is bound by some 38 to 45 kJ/mol, hence barely enough to make up for the entropy loss in the adsorption step. The energy barrier to insertion, relative to the π complex, was calculated to 43 and 55 kJ/mol, depending on the cluster model used. Interaction with a displaceable oxygen donor from the surface, e.g., a siloxane bridge, may decrease the stability of the precursor π complex, possibly enough to render free ethylene and **5a** the proper resting state of the system.

In recent theoretical analyses of the carbonyl IR spectra of the Cr/silica system (5), we found that carbonyl complexes of dinuclear cluster models were able to account for the evolution of the so-called low-temperature triplet with CO pressure. The observed absence of this low-temperature triplet upon short-time polymerization (29), supports dinuclear sites as active for polymerization. Furthermore, as the dinuclear sites may be activated without surface silanol groups, we expect these sites to be responsible for the observed activity in catalysts where all hydroxyl groups have been removed, e.g., fluorinated catalysts (8, 10). Since the latter system produces high molecular weight (MW) polymer, it appears that dinuclear sites may be responsible for the high MW fraction from Phillips catalysts prepared in standard manner (10). This leaves the low MW polymer to be produced by mononuclear sites, and the presence of both kinds of active sites would then contribute toward the broad MW distribution of the polymer produced by conventional Phillips catalysts.

Finally, we note that the presently proposed cyclic intermediates do not introduce methyl nor vinyl end groups to the growing polymer, in agreement with the lack of observation of such during polymerization (8).

6. CONCLUSION

A dichromium site is found to react with ethylene to provide a viable starting structure for polymerization, without external sources of hydrogen. The initiation reaction may proceed *via* the formation of a chromacyclopentane species, to be rearranged to a μ-butano-μ-oxo-dichromium(III) species through migration of an α-carbon to the adjacent Cr(II) center. Ethylene coordinates to either of the resulting trivalent chromium centers and inserts into a Cr–C bond with a reaction barrier compatible with high catalytic activity. The dinuclear site is predicted to form 1-hexene selectively during the early stages of polymerization, without introduction of hydrogen atoms foreign to the monomers.

ACKNOWLEDGMENTS

The Research Council of Norway supported this research financially and through a grant of computing time (Programme for Supercomputing). Para//ab High Performance Computing Centre, Bergen, Norway, is thanked for extensive amounts of computer time.

REFERENCES

1. Thüne, P. C., Verhagen, C. P. J., van den Boer, M. J. G., and Niemantsverdriet, J. W., *J. Phys. Chem. B* **101**, 8559 (1997).
2. Weckhuysen, B. M., and Schoonheydt, R. A., *Catal. Today* **51**, 215 (1999).
3. Scott, S. L., and Ajjou, J. A. N., *Chem. Eng. Sci.* **56**, 4155 (2001).
4. Espelid, Ø., and Børve, K. J., *Catal. Lett.* **75**, 49 (2001).
5. Espelid, Ø., and Børve, K. J., *J. Catal.* **205**, 177 (2002).
6. Espelid, Ø., and Børve, K. J., *J. Catal.* **195**, 125 (2000).
7. Espelid, Ø., and Børve, K. J., *J. Catal.* **205**, 366 (2002).
8. McDaniel, M. P., *Adv. Catal.* **33**, 47 (1985).
9. McDaniel, M. P., *Ind. Eng. Chem. Res.* **27**, 1559 (1988).
10. McDaniel, M. P., and Welch, M. B., *J. Catal.* **82**, 98 (1983).
11. Ruddick, V. J., and Badyal, J. P. S., *J. Phys. Chem. B* **102**, 2991 (1998).
12. Ghiotti, G., Garrone, E., and Zecchina, A., *J. Mol. Catal.* **46**, 61 (1988).
13. Zecchina, A., Spoto, G., Ghiotti, G., and Garrone, E., *J. Mol. Catal.* **86**, 423 (1994).
14. Kohler, S. D., and Ekerdt, J. G., *J. Phys. Chem.* **98**, 4336 (1994).
15. Rebenstorf, B., *J. Polym. Sci. Pol. Chem.* **29**, 1949 (1991).
16. Thüne, P. C., Linke, R., van Gennip, W. J. H., de Jong, A. M., and Niemantsverdriet, J. W., *J. Phys. Chem. B* **105**, 3073 (2001).
17. Rebenstorf, B., and Larsson, R., *J. Mol. Catal.* **11**, 247 (1981).
18. Baerends, E. J., Bérces, A., Bo, C., Boerrigter, P. M., Cavallo, L., Deng, L., Dickson, R. M., Ellis, D. E., Fan, L., Fischer, T. H., Fonseca Guerra, C., van Gisbergen, S. J. A., Groeneveld, J. A., Gritsenko, O. V., Harris, F. E., van den Hoek, P., Jacobsen, H., van Kessel, G., Kootstra, F., van Lenthe, E., Osinga, V. P., Philipsen, P. H. T., Post, D., Pye, C. C.,

Ravenek, W., Ros, P., Schipper, P. R. T., Schreckenbach, G., Snijders, J. G., Sola, M., Swerhone, D., te Velde, G., Vernooijs, P., Versluis, L., Visser, O., van Wezenbeek, E., Wiesenekker, G., Wolff, S. K., Woo, T. K., and Ziegler, T., ADF 2000.02 Computer Code (2000).
19. Guerra, C. F., Snijders, J. G., te Velde, G., and Baerends, E. J., *Theor. Chem. Acc.* **99**, 391 (1998).
20. Vosko, S. H., Wilk, L., and Nusair, M., *Can. J. Phys.* **58**, 1200 (1980).
21. Perdew, J. P., *Phys. Rev. B* **33**, 8822 (1986).
22. Becke, A. D., *Phys. Rev. A* **38**, 3098 (1988).
23. Jensen, V. R., and Børve, K. J., *J. Comput. Chem.* **19**, 947 (1998).
24. Weckhuysen, B. M., Wachs, I. E., and Schoonheydt, R. A., *Chem. Rev.* **96**, 3327 (1996).
25. Krauss, H.-L., and Stach, H., *Z. Anorg. Allg. Chem.* **366**, 280 (1969).
26. Liu, B., and Terano, M., *J. Mol. Catal. A* **172**, 227 (2001).
27. Espelid, Ø., Børve, K. J., and Jensen, V. R., *J. Phys. Chem. A* **102**, 10414 (1998).
28. Isaacs, N. S., *in* "Physical Organic Chemistry," Chap. 8, p. 283. Longman, New York, 1995.
29. Rebenstorf, B., *Z. Anorg. Allg. Chem.* **571**, 148 (1989).
30. Krauss, H.-L., and Hums, E., *Z. Naturforsch.* **34B**, 1628 (1979).